Dugdale, S. B., & Laverock, J. (2014). Recovering the Fermi surface with 2D-ACAR spectroscopy in samples with defects. Journal of Physics: Conference Series, 505(1), 1 - 5. [012046]. 10.1088/1742-6596/505/1/012046

Recovering the Fermi surface with 2D-ACAR spectroscopy in samples with defects

2014 J. Phys.: Conf. Ser. 505 012046

(http://iopscience.iop.org/1742-6596/505/1/012046)

Journal of Physics: Conference Series **505** (2014) 012046 doi:10.1088/1742-6596/505/1/012046

Recovering the Fermi surface with 2D-ACAR spectroscopy in samples with defects

SB Dugdale[1] and J Laverock[2]

[1]HH Wills Physics Laboratory, University of Bristol, Tyndall Avenue, Bristol BS8 1TL, UK
[2]Department of Physics, Boston University, 590 Commonwealth Avenue, Boston, Massachusetts 02215, USA

E-mail: s.b.dugdale@bristol.ac.uk

Abstract. When two-dimensional angular correlation of positron annihilation radiation (2D-ACAR) experiments are performed in metals containing defects, conventional analysis in which the measured momentum distribution is folded back into the first Brillouin zone is rendered ineffective due to the contribution from positrons annihilating from the defect. However, by working with the radial anisotropy of the spectrum, it is shown that an image of the Fermi surface can be recovered since the defect contribution is essentially isotropic.

Introduction

As a probe of the Fermi surface, positron annihilation occupies an important place in the array of probes which include quantum oscillations [1], angle-resolved photoemission [2] and the closely related technique of Compton scattering [3, 4, 5]. When a positron annihilates with an electron in a metal, the predominant process produces two γ-ray photons which, due to momentum conservation, are emitted almost anti-parallel in the laboratory frame. It can be shown that measurement of the angular distribution of the photons' deviations from anti-collinearity is equivalent to a measurement of the projection of the electron-positron momentum distribution along an axis perpendicular to the mean emission axis of the measurement. The full three-dimensional momentum density can be reconstructed, if necessary, using tomographic techniques [6, 7, 8]. Since the positron has a Maxwell-Boltzmann thermal momentum (with a typical radioisotope source activity, there is only one positron in the sample at any time), the pair momentum is dominated by that of the electron. While the principal strengths of the positron technique, conventionally referred to as two-dimensional angular correlation of positron annihilation radiation (2D-ACAR) spectroscopy, include its bulk sensitivity, the k-resolved nature of the obtained spectra and its insensitivity to the electronic mean-free-path (meaning that substituionally disorded alloys and high-temperature phases are accessible), the fact that the positron is positively charged means that it is energetically favourable for it to become trapped at vacancy-type defects. The fate of a positron on entering a metal containing vacancies depends to a large extent on the concentration and distribution of those vacancies. After rapid thermalization (typically on a timescale of a few ps), in a defect free metal the positron diffuses through the crystal with a diffusion length of the order of ~ 1000Å. Thus whether it encounters a vacancy and consequently becomes trapped depends on the concentration of vacancies. Once trapped, the positron, which was formerly in a delocalized (Bloch) state, is localized at the defect

site leading to wavefunctions which are almost isotropic [9]. As pointed out by Prasad *et al.* [10], translational symmetry is destroyed by the presence of a vacancy so that *all* occupied electron states contribute to the momentum distribution. This should be contrasted with the bulk case in which a Bloch-state positron which annihilates with an electron with crystal momentum $\mathbf{k}$ will contribute to the momentum distribution only at momenta $\mathbf{p} = \mathbf{k} + \mathbf{G}$, where $\mathbf{G}$ is a reciprocal lattice vector. In this case the momentum distribution will reflect the anisotropy of the bulk electronic structure and Fermi surface, whereas in the presence of vacancy-type defects this anisotropy is washed out to varying extents depending on what fraction of positrons are trapped. In the case of saturation trapping, when all positrons implanted into the material are trapped, the momentum distribution is very isotropic, leaving no hope of extracting any information about the bulk Fermi surface. In this paper we focus on the intermediate regime where not all positrons are trapped and some anisotropy remains, and show that even at relatively high trapped positron fractions it is still possible to infer the bulk Fermi surface.

For Fermi surface studies, except for the simplest of topologies, a direct interpretation of the measured momentum- (that is real momentum, $\mathbf{p}$-) space spectra is difficult since the signatures of the Fermi surface (the discontinuities in the momentum distribution) are widely distributed across the spectrum since an electron with crystal momentum $\mathbf{k}$ will contribute not only at $\mathbf{p} = \mathbf{k}$, but also, as mentioned above, at $\mathbf{p} = \mathbf{k} + \mathbf{G}$. Moreover, these signatures are themselves difficult to see in the raw spectra, not least because of the projected nature of the measured spectra. In the early days of two-dimensional measurements it was commonplace to subtract an isotropic distribution (either a fitted gaussian or the simple angular average of the spectrum itself) from the measured spectrum, $N(p_x, p_y)$. This is often referred to as the radial anisotropy, $R(p_x, p_y)$, and is defined as

$$R(p_x, p_y) = N(p_x, p_y) - \overline{N(p_x, p_y)}|_{p=\text{const.}} \tag{1}$$

This procedure is still routinely performed during experiments to check that the sample has been properly aligned. However, Lock, Crisp and West had already pointed out that a translationally invariant distribution in crystal momentum- ($\mathbf{k}$-) space could be constructed by 'folding' the real momentum ($\mathbf{p}$)-space distribution back into the the first Brillouin zone by translating those $\mathbf{p}$ points by an appropriate reciprocal lattice vector [11]. For a purely electron momentum distribution within the independent particle model (IPM), this procedure results in the contribution from full bands being constant across the Brillouin zone, and the contributions from partially filled bands reinforcing each other to give step-function-like changes in occupation at the Fermi surface. For positrons, although this 'LCW theorem' is only approximate (even within the IPM), the contributions of the occupied bands nevertheless sum to give a smoothly varying background on top of which the contributions of the partially occupied bands also sum, with the Fermi surface breaks being put back together on top of each other. However, in the situation where some fraction of the positrons are trapped and annihilate from the vacancy, they contribute an (almost) isotropic momentum distribution which is superimposed on the bulk distribution due to untrapped positrons. This extra component makes conventional LCW analysis dangerous, since this peaked defect contribution is likely to dominate the structure of the LCW spectrum. Similar problems can also arise in the reconstruction of the three-dimensional momentum distribution after the application of tomographic procedures, with methods involving an explicit Fourier transform being particularly prone to spurious peaks at low momentum [12, 13]. In fact, this is one of the major reasons for the Bristol group preferring the Cormack method for reconstruction [6, 14, 15, 16].

As mentioned earlier, within the IPM, the LCW 'theorem' applied to the electron momentum distribution is exact since the electronic wavefunctions are orthogonal and normalized. One can immediately grasp what the LCW process is doing in folding back the higher momentum

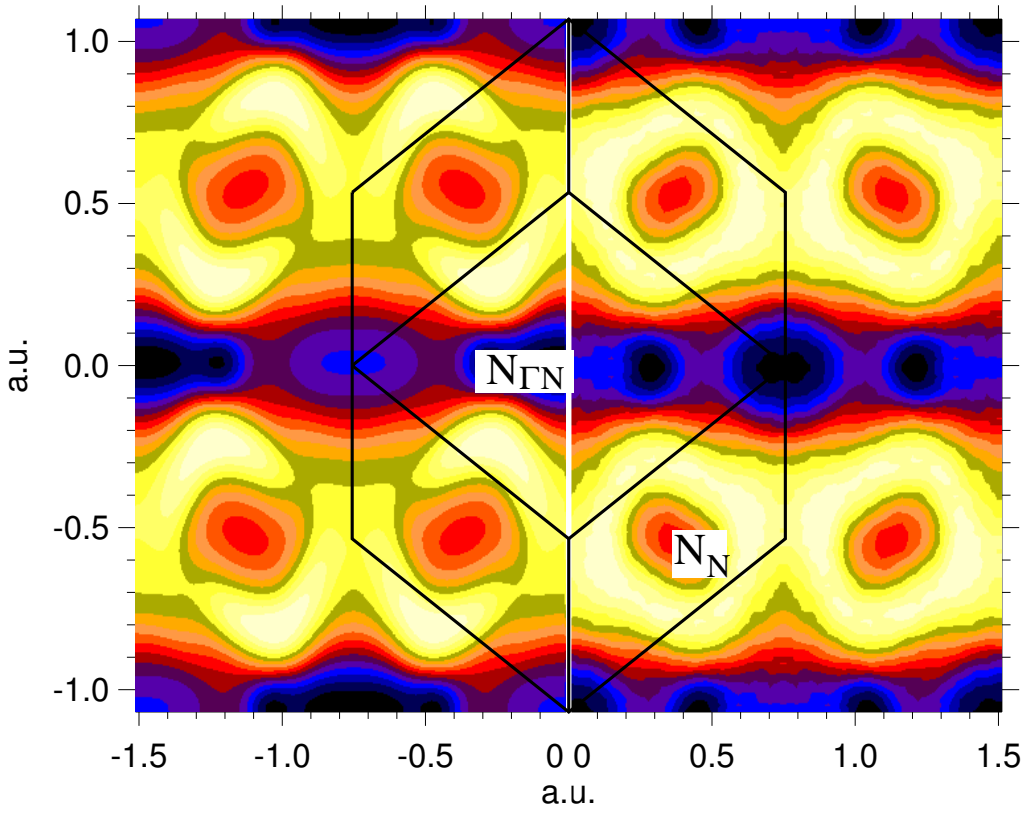

Figure 1. Projected [110] Brillouin zone occupancy of V (horizonal axis is $[1\bar{1}0]$ and vertical axis is [001] obtained from an electronic structure calculation (left hand side of figure) and measured LCW spectrum from experiment (right hand side of figure). Some (projected) high symmetry points are labelled and the (projected) Brillouin zone is indicated.

components ('Umklapps') back into the first Brillouin zone. Moreover, in the case of electron-positron momentum distributions, as long as the **k**-dependence of the positron wavefunction is weak, the modulations introduced are likely to be small, and in any case the breaks associated with the presence of the Fermi surface in the electron distribution remain.

Here we show that in fact if one is only interested in seeing the occupied regions of the Brillouin zone, and hence the shape of the Fermi surface, then it is possible to apply the LCW folding procedure not to the momentum distribution itself, but to its radial anisotropy. This has the advantage that if there is a contribution from defects which is (almost) isotropic, then this will not appear in the radial anisotropy distribution and will thus be excluded from the subsequent LCW summation. We illustrate this with reference to a 2D-ACAR experiment on V in which the data are projected down the [110] crystallographic direction (details of the experiment can be found in Ref. [17]). In Fig. 1 the LCW distribution is shown together with an occupancy extracted from a calculation performed using the ELK electronic structure code [18]. As is expected, the LCW distribution broadly reflects the occupancy of the Brillouin zone with the differences principally due to the perturbations introduced by the positron wavefunction [19].

In Fig. 2, a series of LCW distributions are shown to illustrate the effect of adding an (isotropic) gaussian component to represent the presence of a contribution from positrons trapped at defects. At a relatively small defect contribution (with only 1% of positrons being

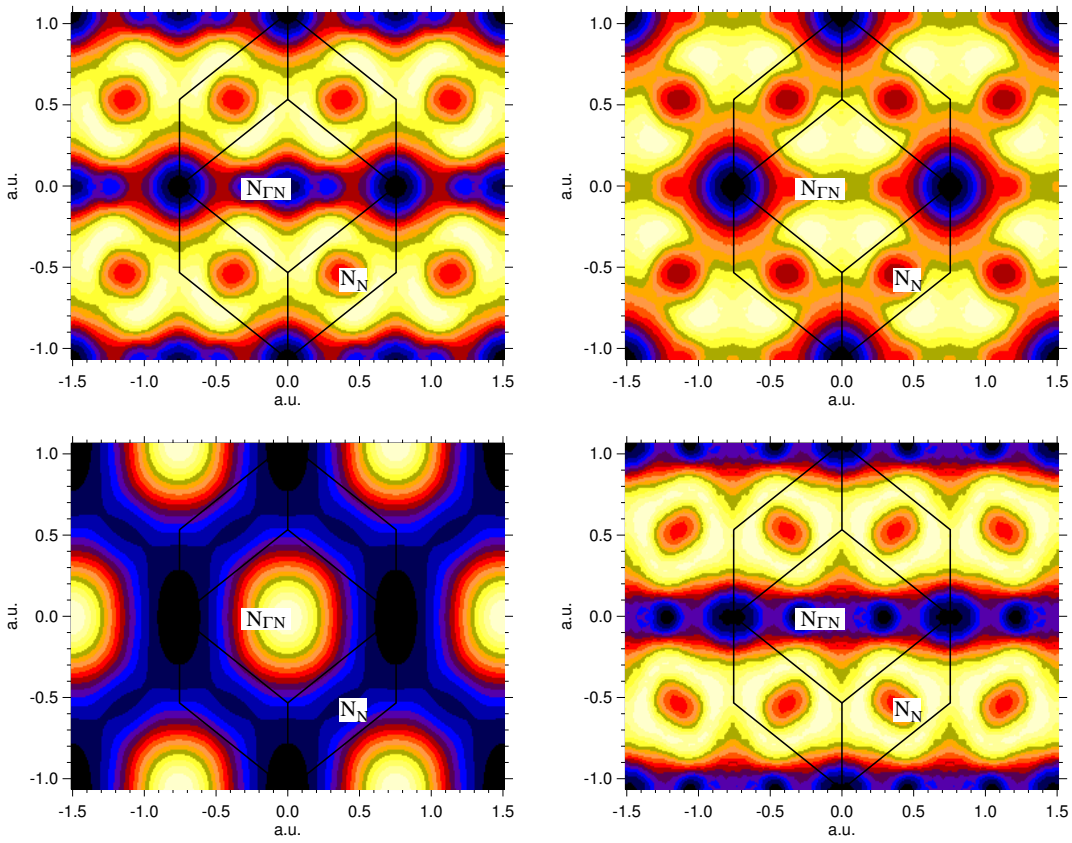

Figure 2. Series of LCW distributions on data with simulated defect component. The fraction of positrons annihilating from the trapped state are 1% (top left), 5% (top right) and 33% (bottom left). The final distribution (bottom right) is the LCW of the radial anisotropy.

trapped), there is little deleterious impact on the LCW distribution (top left). However, with higher positron trapping (5% (top right) and 33% (bottom left)), it is very obvious that the LCW distributions can no longer be relied upon to indicate the Fermi surface, with the 33% distribution unrecognizably different from the occupancy. However, the LCW distribution of the radial anisotropy is, of course, insensitive to the presence of a large isotropic defect contribution (apart from the negative effect on the signal-to-noise ratio). In the bottom right panel of Fig. 2 this radial anisotropy LCW distribution is shown (actually for the 33% trapping) and is clearly very similar to those in Fig. 1. This is because the radial anisotropy procedure emphasizes the anisotropy of the data which is always partly due to the presence of the Fermi surface (in addition to general wavefunction anisotropy) and the LCW folding constructively reinforces these Fermi surface signatures. We believe that it is likely to be applicable whenever the contribution to the momentum distribution from trapped positrons is isotropic.

It is, however, a little surprising just how effective this procedure is. In multiband systems (for it is often in these kinds of materials, for example charge-density-wave systems [20, 21, 22], where the **k**-resolved nature of positron annihilation can make substantial contributions) it is often difficult to disentangle the Fermi surface information from a single projection without the assistance of a theoretical calculation, as pointed out by [23], and when the signals are weak due to either limited positron overlap, or the sheer number of occupied bands it is important to find ways of making the most of your data. The sensitivity of the radial anisotropy to the shape of

the Fermi surface (in many cases) was exploited by Major *et al.* [24] who sought to compare the measured radial anisotropies to those from electronic structure calculations [25]. Spurred on by the challenge posed by strong wavefunction effects and small Fermi surface signals in the early days of cuprate superconductivity, several groups were working on image processing methods [26] designed to emphasize the Fermi surface signatures, and it is notable that a kind of 'difference' LCW was used at that time [17], albeit for a different purpose. In the closely related field of Compton scattering, we have also previously used the anisotropic part of the reconstructed momentum distribution in our work on Co-doped $BaFe_2As_2$ [3], and it also appears to be used by other groups [27]. This approach is also likely to be more generally useful for removing Fourier-based-reconstruction artefacts.

Conclusions

In the circumstance of having made a 2D-ACAR measurement on a sample which contains vacancy-type defects in which some fraction of the positrons have been trapped, the LCW folding of the radial anisotropy appears to be a viable route towards accessing the bulk Fermi surface. With new 2D-ACAR spectrometers coming online [28, 29], this technique may prove very useful. Finally we would like to emphasise that we make no claims about these 'radial anisotropy' LCW distributions beyond the statement that this kind of analysis appears to give sensible Fermi surface information in the case of a measurement which contains a contribution from annihilation in defects.

References

[1] Ru N *et al.* 2008 *Phys. Rev. B* **78**(4) 045123
[2] Brouet V *et al.* 2008 *Phys. Rev. B* **77**(23) 235104
[3] Utfeld C *et al.* 2010 *Phys. Rev. B* **81**(6) 064509
[4] Laverock J *et al.* 2007 *Phys. Rev. B* **76**(5) 052509
[5] Dugdale S B *et al.* 2006 *Phys. Rev. Lett.* **96** 046406
[6] Kontrym-Sznajd G 1990 *Phys. Stat. Sol. A* **117** 227
[7] Major Z *et al.* 2004 *Phys. Rev. Lett.* **92** 107003
[8] Haynes T D *et al.* 2012 *New Journal of Physics* **14** 035020
[9] Puska M J and Nieminen R M 1983 *Journal of Physics F: Metal Physics* **13** 333
[10] Prasad R, Benedek R, Robinson J E and Bansil A 1989 *Phys. Rev. B* **40**(13) 8620–8630
[11] Lock D G, Crisp V H C and West R N 1973 *Journal of Physics F: Metal Physics* **3** 561
[12] Fretwell H M *et al.* 1995 *Europhysics Lett.* **32** 771–776
[13] Pecora L M *et al.* 1988 *Phys. Rev. B* **37**(12) 6772–6782
[14] Cormack A M 1963 *Journal of Applied Physics* **34** 2722–2727
[15] Cormack A M 1964 *Journal of Applied Physics* **35** 2908–2913
[16] Crowe S J *et al.* 2004 *Europhysics Lett.* **65** 235–241
[17] Dugdale S B *et al.* 1994 *Journal of Physics: Condensed Matter* **6** L435–L443
[18] URL `http://elk.sourceforge.net/`
[19] Laverock J, Haynes T D, Alam M A and Dugdale S B 2010 *Phys. Rev. B* **82** 125127
[20] Laverock J, Dugdale S B, Major Z, Alam M A, Ru N, Fisher I R, Santi G and Bruno E 2005 *Phys. Rev. B* **71** 085114
[21] Laverock J, Haynes T D, Utfeld C and Dugdale S B 2009 *Phys. Rev. B* **80**(12) 125111
[22] Mansart B *et al.* 2012 *Proceedings of the National Academy of Sciences* **109** 5603–5608
[23] Rabou L and Mijnarends P 1984 *Solid State Communications* **52** 933 – 936
[24] Major Z *et al.* 2004 *J. Phys. Chem. Solids* **65** 2011
[25] Barbiellini B, Dugdale S B and Jarlborg T 2003 *Comp. Mater. Sci.* **28** 287–301
[26] O'Brien K M, Brand M Z, Rayner S and West R N 1995 *Journal of Physics: Condensed Matter* **7** 925
[27] Barbiellini B 2013 *Journal of Physics: Conference Series* **443** 012009
[28] Ceeh H *et al.* 2013 *Review of Scientific Instruments* **84** 043905
[29] Dugdale S B, Laverock J, Utfeld C, Alam M A, Haynes T D, Billington D and Ernsting D 2013 *Journal of Physics: Conference Series* **443** 012083